ACS APPLIED POLYMER MATERIALS

pubs.acs.org/acsapm

Article

Preparation of Sodium Carboxymethyl Cellulose–Chitosan Complex Membranes through Sustainable Aqueous Phase Separation

Lijie Li, Muhammad Irshad Baig, Wiebe M. de Vos, and Saskia Lindhoud*

Cite This: *ACS Appl. Polym. Mater.* 2023, 5, 1810–1818

Read Online

ACCESS | Metrics & More | Article Recommendations | Supporting Information

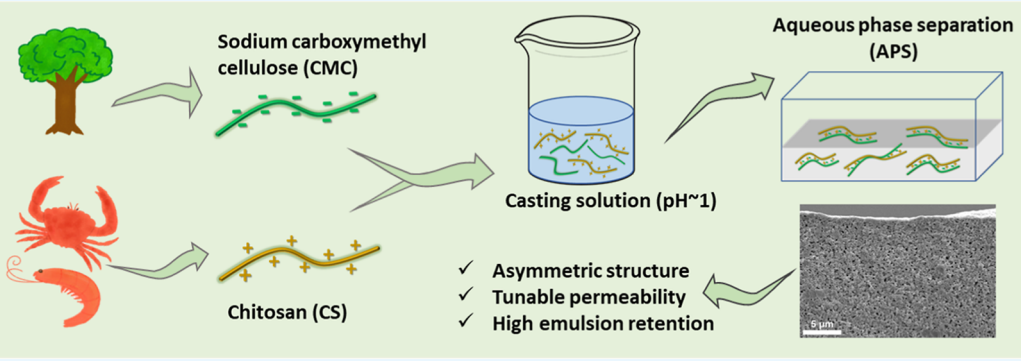

ABSTRACT: The aqueous phase separation (APS) technique has recently been introduced as one of the more sustainable methods to produce polymeric membranes. So far, almost all the APS membranes are produced on the basis of synthetic polyelectrolytes that are typically obtained from petroleum sources. In this work, we utilized natural polyelectrolytes to produce even more sustainable membranes via APS. Two natural polyelectrolytes, polyanionic sodium carboxymethyl cellulose (CMC) and polycationic chitosan (CS), were used to fabricate the polyelectrolyte complex membranes. By changing the solution pH and monomer ratio of polyelectrolytes, a desired homogeneous casting solution was prepared at pH ∼1 where CMC was uncharged. Exposing this solution to an acetate buffer coagulation bath at pH ∼5 caused CMC to acquire negative charges, leading to the formation of a polyelectrolyte complex with the positively charged CS. The structure and properties of the resultant membranes could be tuned by changing the concentration and pH of the acetate buffer. All the membranes showed an asymmetric structure with a dense top layer and porous inner structure. The membranes possessed tunable pure water permeability and were able to effectively (∼99%) remove oil droplets from an oil-in-water emulsion. This work demonstrates that natural polyelectrolytes can indeed be used to produce more sustainable APS membranes that can be directly applied for water treatment.

KEYWORDS: *natural polyelectrolytes, complex, membranes, aqueous phase separation, microfiltration*

1. INTRODUCTION

Due to their highly versatile separation properties and relatively low energy demand, membranes have been widely used in agriculture, industry, and medicine, for example, for wastewater treatment, gas separation, and drug delivery.[1−3] Since the 1960s, the nonsolvent-induced phase separation (NIPS) approach has played a dominant role in polymeric membrane production. In NIPS, polymers are dissolved in organic solvents and precipitated in nonsolvent baths to induce phase separation, leading to the formation of polymeric membranes. Unfortunately, the commonly used organic solvents in NIPS, like *N*-methyl-pyrrolidone and *N*,*N*-dimethylformamide, are unsustainable and toxic to the environment and humans.[4] To solve this problem, methods that use less-toxic solvents have been proposed to prepare the polymeric membranes.[5]

Polyelectrolytes are water-soluble polymers with chargeable groups making them either positively or negatively charged. When two oppositely charged polyelectrolytes are mixed, an associative solid called a polyelectrolyte complex can form.[6] However, if the polyelectrolytes are mixed under conditions where one of the polyelectrolytes is uncharged, that is, at a high pH for weak polybases or low pH for weak polyacids, or when the ionic strength is sufficiently high, no polyelectrolyte complexation will occur. This property of polyelectrolytes has been utilized to prepare polyelectrolyte complex membranes by a completely aqueous approach, that is, aqueous phase separation (APS).[7−13] Indeed, our group has recently

Received: October 31, 2022
Accepted: January 31, 2023
Published: February 9, 2023

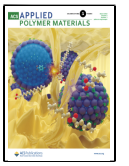

successfully demonstrated the use of APS for various membrane types and from several different polyelectrolyte pairs.[7−9,13] There are two approaches to achieving phase separation in the APS process. The first one is the pH-change-induced APS where a polyelectrolyte solution is first obtained by mixing a strong and a weak polyelectrolyte at a pH where the latter is uncharged. The solution is then cast on a glass plate and immersed in a coagulation bath at a pH where the weak polyelectrolyte acquires charges and forms a porous polyelectrolyte complex membrane with the strong polyelectrolyte.[9,13−15] The second approach is the salinity change-induced APS, where the excess ions in the casting solution can eliminate the entropic driving force for complexation between the two oppositely charged strong polyelectrolytes. Immersing the high-salinity polyelectrolyte solution in a low-salt-concentration water bath causes the salt to diffuse out of the solution, resulting in the formation of a polyelectrolyte complex membrane.[8,10−12] Compared to NIPS, the whole membrane fabrication process uses water as both the solvent and the nonsolvent. It has been successfully demonstrated that membranes with controllable structures and filtration performance can be produced via the APS approach. However, until now, only petroleum-based polyelectrolytes have been used in the APS method, and one could argue that this is not yet truly sustainable.

Bio-based polyelectrolytes are good alternatives to petroleum-based polyelectrolytes because of their well-sourced, nontoxic, biodegradable, and biocompatible properties. During the past 10 years, various bio-based polyelectrolytes such as chitosan (CS),[16] alginates,[17] pectin,[18] dextran,[19] cellulose, and its derivatives[20] have been successfully used to prepare membranes and have already been applied in different applications in food,[21] medicine,[22] and environment.[23] Among many natural polyelectrolytes, CS is the most abundant cationic polymer and has been widely researched.[24−26] CS is produced by the deacetylation of chitin and has film-forming and antibacterial properties.[27,28] Tu et al. recently fabricated CS membranes via the APS approach through the CS gelation, and they used an optical coherence tomography technique to study the gelation kinetics of the membranes, which gave more understanding of the APS approach based on natural polymers.[29] On the other hand, different polyanionic biopolymers, such as sodium carboxymethyl cellulose (CMC), a common cellulose derivative with a carboxymethyl group in its structure, have been combined with CS to prepare multifunctional membranes. CMC is a water-soluble polyanion, and its solution also has good film-forming properties. In addition, it can strongly interact with CS due to their structural similarity.[30]

In the past decades, CMC−CS composite membranes with diverse properties and applications have been developed through different methods. Using the layer-by-layer method, Park et al. built chemical crosslinked multilayer nanofilms using CMC and CS. The drug loading and release from the films were well controlled.[31] Chen et al. prepared CMC−CS blend membranes for lysozyme adsorption by the solution casting and evaporation approach, with glutaraldehyde as a crosslinking agent and silica particles as porogens.[32] Zhao et al. used CMC and CS to prepare solid polyelectrolyte complexes and then dissolved the complexes in aqueous sodium hydroxide to prepare complex membranes by solution casting and evaporation.[33] Besides, freeze-drying and electrostatic spinning are also used to prepare membranes based on CMC and CS.[34,35] However, these methods either need support materials or significant time and/or energy consumption. Therefore, it is promising to use the APS technique to fabricate free-standing membranes via the one-step way without the use of organic solvents.

In this work, the natural polyelectrolytes CMC and CS are utilized to produce free-standing PEC membranes in a single step via the APS method. The pH of the solution and the monomer ratio of CMC and CS were varied to obtain an optimal and desired homogeneous casting solution, which was cast and immersed in an acetate buffer bath to induce phase separation, forming the complex membranes. During this process, acetate buffers of different concentrations and pHs were used to investigate the influence on the final membrane properties. For this, the membrane structure was studied using scanning electron microscopy (SEM), while the pure water permeability and retention of an oil-in-water emulsion were tested to determine their relevance for water treatment.

2. EXPERIMENTAL SECTION

2.1. Materials. Sodium CMC (Mw ∼90 kDa, degree of substitution ∼0.7), CS (Mw ∼50−190 kDa, deacetylation ≥75%), hydrochloric acid (HCl, 37%), acetic acid, sodium acetate, *n*-hexadecane, sodium dodecyl sulfate (SDS), and Oil Red EGN dye were purchased from Sigma-Aldrich, The Netherlands. Ultrapure deionized water from the Advantage A10 purification system (Millipore) was used in all the experiments.

2.2. Preparation of the Casting Solution. CMC solutions (5 wt %) were prepared by directly dissolving CMC in deionized water under constant stirring. On the other hand, CS solutions (5 wt %) were prepared by dissolving CS in diluted HCl solution. The weight percentage of HCl to the CS solution was varied from 0.5 to 4.0 wt % to investigate the best ratio. After sufficient dissolution, the two solutions were mixed in a CMC/CS monomer molar ratio ranging from 2:1 to 1:2. The monomer molar ratios were calculated according to the repeat unit weight of the CMC (218 g·mol^{-1}) and CS (169 g·mol^{-1}) monomers. The mixtures were stirred until a homogeneous solution was obtained, which was left to degas to remove the bubbles.

2.3. Preparation of Polyelectrolyte Complex Membranes. The obtained homogeneous casting solution was cast as a thin film on a glass plate using a casting bar (gap ∼0.6 mm). The glass plate was then immersed in an acetic acid-sodium acetate buffer bath to induce phase separation. Here, the acetate buffer solutions of different concentrations (0.1, 0.5, and 1.0 M, at pH 5) and different pHs (pH 4.5, 5.0, and 5.5, at 0.5 M) were prepared to study the influence on the resulting membrane structure and performance. The resultant membranes were kept in the coagulation bath overnight, taken out the next day, and washed thoroughly with deionized water. Finally, the membranes were stored in deionized water for further characterization.

2.4. Characterization. *2.4.1. Viscosity Measurements.* The viscosity of polyelectrolyte solutions was measured using a HAAKE Viscotester 550 Rotational Viscometer (ThermoFisher Scientific, USA). The solution (∼15 mL) was poured into the spindle cylinder (SV-DIN) first and then mounted on the viscometer. The dynamic viscosity of the solution was measured as a function of the shear rate (Υ = 1.1−258 s^{-1}) at 25 °C.

2.4.2. Characterization of Membrane Structure. The surface and cross-sectional morphologies of the membranes were characterized by SEM (JSM6010LA, JEOL, Japan). The membranes were first placed in a 20 wt % glycerol solution overnight and then dried in a fume hood. For cross-sectional images, the glycerol-dried membranes were immersed in liquid nitrogen, followed by quick fracturing to prepare samples with intact pore structures. After vacuum drying at 30 °C for 24 h, the samples were coated with a 5 nm layer Pt/Pd using a Quorum Q150T ES sputter coater before taking SEM images. The

https://doi.org/10.1021/acsapm.2c01901
ACS Appl. Polym. Mater. 2023, 5, 1810−1818

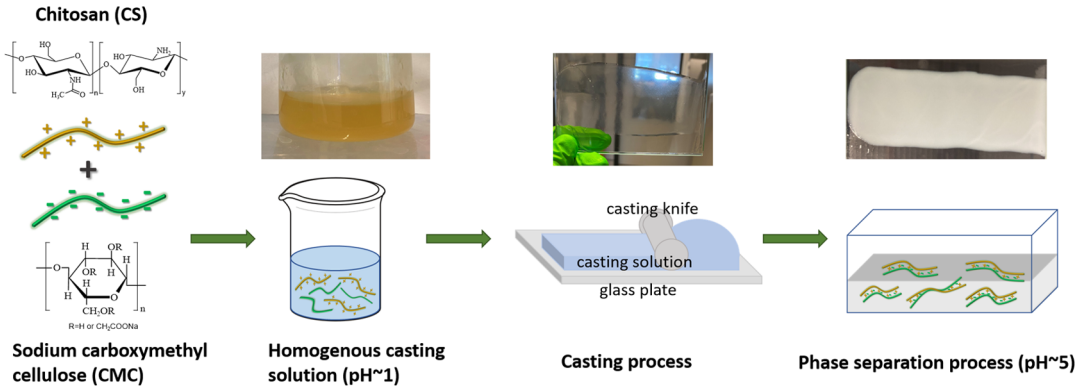

Figure 1. Schematic illustration of the CMC−CS membrane preparation process through the APS method.

membrane pore diameter was calculated by analyzing the top-surface SEM images using ImageJ software.

2.4.3. Pure Water Permeability Test. The prepared membranes were cut into circles with a diameter of approximately ∼2.5 cm. The cut samples were mounted on a dead-end filtration setup, and nitrogen gas (pressure ∼1 bar) was used to pressurize the feed water. The permeate was collected, and the mass was measured as a function of time to give the water flux (J_w). A minimum of three samples were measured for each membrane. The pure water permeability (P) was calculated using eq 1

$$P = \frac{J_W}{\Delta p} \tag{1}$$

where J_w is the water flux ($L{\cdot}m^{-2}{\cdot}h^{-1}$) and Δp is the transmembrane pressure (bar).

2.4.4. Oil-in-Water Emulsion Retention Test. The same dead-end filtration setup as described above was used to test the retention performance of the membranes against an oil-in-water emulsion. The emulsion was prepared via the protocol mentioned elsewhere.[13,36] Briefly, *n*-hexadecane (100 $mg{\cdot}L^{-1}$) was mixed with Oil Red EGN dye (20 $mg{\cdot}L^{-1}$) and gradually added to SDS solution (463 $mg{\cdot}L^{-1}$) under constant stirring at 14,000 rpm. The emulsion was stirred continuously for 20 min. Here, the oil-soluble dye was added as a simple marker for the emulsion droplets. Following this protocol, an emulsion having an oil droplet size of 3−4 μm was obtained.[36] The separation test was conducted at a feed pressure of 1 bar. The permeate solutions were collected and analyzed using a PerkinElmer Lambda 850 UV−vis spectrophotometer at λ_{max} = 521 nm, which is the maximum absorbance wavelength of Oil Red EGN. At least three samples were tested, and the retention R (%) was calculated using the following equation

$$R = \frac{C_f - C_p}{C_f} \times 100 \tag{2}$$

where C_f and C_p are the concentration of the oil droplets in the feed and the permeate solutions, respectively.

3. RESULTS AND DISCUSSION

Recently, the APS approach has been successfully used to prepare polyelectrolyte complex membranes. In this approach, water is used as both the solvent and the nonsolvent. A change in pH or ionic strength is used to regulate the charge on one or both polymers, respectively.[7−9] Here, membranes of two natural, green polyelectrolytes were made via the pH-shift-induced APS technique. The polyelectrolyte casting solution was first prepared using CMC and CS at a low pH, where the former was uncharged. After casting, the film was submerged in a bath at high pH, where CMC acquired negative charges, thus forming a water-insoluble polyelectrolyte complex with the positively charged CS. The membrane production process is schematically shown in Figure 1.

3.1. Preparation of the Casting Solution. In the APS approach, the ideal casting solution should have a suitable viscosity, enough polymer concentration to give the formed membranes strength, and more importantly, no complexation between the polyelectrolytes.[14] The aqueous CS solutions have a significantly high viscosity already at a relatively low molecular weight and polymer concentrations.[37] Therefore, to obtain a fluid solution, a low-molecular-weight CS (50−190 kDa) at a 5 wt % concentration was prepared. Additionally, CS is usually dissolved under acidic conditions with a pKa of 6;[38] therefore, the pH range at which CS is soluble was investigated first by adding HCl to the solution (see Figure S1). At extremely low concentrations of HCl such as at 0.5 wt %, a highly viscous gel was obtained because the acid content was not sufficient to completely protonate the CS. As a result, some polyelectrolyte chains can exist in their uncharged coiled state, resulting in a highly viscous gel. When the HCl concentration was increased to 1.0 wt %, CS began to fully dissolve because of the adequate protonation of amino groups, leading to a relatively fluid solution having a dynamic viscosity of ∼47 Pa·s (Υ = 1.1 s^{-1}, 25 °C). With further increase in the HCl concentration to 1.5 wt % and then to 2 wt %, the solubility of CS improved slightly, which is evident by the decreasing viscosity of the CS solutions, that is, ∼34 and ∼31 Pa·s, respectively. However, at extremely high amounts of HCl such as 2.5, 3.0, and 4.0 wt %, CS solutions began to display two separated phases, perhaps because the excess HCl led to the salting-out effect that is associated with polyelectrolytes.[39] The relatively high solubility and lower viscosity obtained at 2 wt % HCl result in a pH of approximately 1. This CS solution was used for further experiments.

The CS solution was mixed with the CMC solution in different monomer ratios to obtain the casting solutions, see the photographs in Figure S2. When the concentration of CMC was higher than that of CS, for example, 2:1, the resultant mixture phase separated to form a coacervate having a polymer-rich and a polymer-lean phase. It was most likely because the pH of the mixture was not sufficiently low to completely protonate the CMC. Some CMC was expected to be partly charged, which could result in the formation of a complex coacervate with CS. Increasing the CS concentration and thereby lowering the pH below the pKa of CMC (pKa ∼4)[40] could cause the CMC to become more protonated and therefore uncharged, leading to the formation of a clear solution when mixed with CS. However, the solution having a

https://doi.org/10.1021/acsapm.2c01901
ACS Appl. Polym. Mater. 2023, 5, 1810−1818

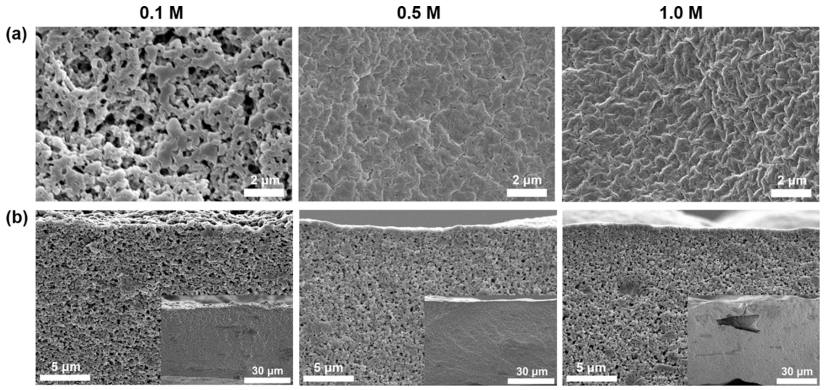

Figure 2. SEM images of the membranes: (a) top surface (10,000× magnification) and (b) cross-section (5000× magnification) prepared at different acetate buffer concentrations (0.1, 0.5, and 1.0 M) in the coagulation bath. The magnifications of the inset images are 1500× (0.1 and 0.5 M) and 1300× (1.0 M). The pH of the buffer bath was kept at 5.

ratio of 1.5:1 started to form microscopic complexes after a few days. Only the solutions with CMC/CS monomer mixing ratios of 1:1, 1:1.5, and 1:2 were homogeneous and therefore used for further processing. The solutions were cast on the glass plates and immediately submerged in the acetate buffer baths (pH ∼5, concentration of 0.5 M), resulting in the membrane formation. It can be seen in Figure S3 that at the 1:1 mixing ratio, a stable and intact membrane was obtained, while at the 1:1.5 and 1:2 ratios, the membranes were broken and significantly shrunk after placing them in water for several hours. Based on the results, the CMC/CS ratio of 1:1 with a solution dynamic viscosity of ∼8 Pa·s ($\Upsilon = 1.1\ s^{-1}$, 25 °C) was selected as the most suitable one for membrane formation. Such a 1:1 ratio would be expected for polyelectrolyte systems where the charged monomers are of roughly equal size, as is the case here, and was, for example, also used previously for PDADMAC-PSS membranes.[8]

3.2. Effect of the Acetate Buffer Concentration. From previous work, we know that the membrane structure can be further optimized by changing the coagulation bath conditions.[9] Since an acetate buffer solution is used as a coagulation bath, the concentration and pH of this buffer are expected to play a significant role in affecting the structure and properties of the resultant membranes. The buffer concentration will influence the membrane structure as it in part determines the kinetics of ion exchange and thus the eventual phase separation. A higher buffer concentration will be expected to lead to faster phase separation due to the larger driving force between the polyelectrolyte solution (pH ∼1) and the buffer bath (pH ∼5). Therefore, the effect of acetate buffer concentration was first investigated by preparing the membranes in different concentrations of the acetate buffer (0.1, 0.5, and 1.0 M, at pH 5).

Figure S4 shows that intact and stable membranes were obtained in all the acetate buffer concentrations. However, the membranes prepared in the 0.1 M bath were relatively less strong and difficult to remove from the glass plates. In addition, the cast film needed a longer time (∼120 s) to complete the complexation and phase separation process. In comparison, the membranes prepared in 0.5 and 1.0 M baths only needed ∼30 and ∼20 s, respectively. This is because the buffer capacity increases at higher buffer concentrations. Higher buffer capacity can well maintain the pH of the coagulation bath, thus the CMC can rapidly acquire the negative charges, causing the fast precipitation rate and polyelectrolyte complexation due to the high pH-change-induced driving force. Meanwhile, the membranes prepared in 0.5 and 1.0 M baths were easily detached from the glass plate as a result of the faster complexation.

The membrane structures were further characterized by SEM. As shown in Figure 2b, all the membranes exhibited asymmetric structures, having a difference in porosity from the top to the bottom. Looking at Figure 2a, it is evident that the top surfaces became denser with an increase in buffer concentration. This is also observed from the cross-sectional images as more obvious dense layers appeared near the top surface. The membrane prepared in a 0.1 M buffer bath had an irregular porous top surface due to the slow speed of the phase separation. With the increase in buffer concentration, the membrane surface pore diameter reduced significantly. The average pore diameter of the membranes prepared in a 0.1 M buffer bath was 231 nm, while the membranes prepared in 0.5 and 1.0 M buffer baths showed average pore diameters of 80 and 89 nm, respectively, see Figure S6. This is consistent with the results of polyethyleneimine-poly (sodium 4-styrene sulfonate) (PEI-PSS) polyelectrolyte membranes prepared by the same APS method, where a high buffer concentration resulted in a denser top surface.[9] However, compared to the PEI-PSS membranes, no finger-like macrovoids were present in the cross-sections of CMC−CS membranes prepared at any concentrations of acetate buffer bath. All the prepared membranes showed a sponge-like morphology. This is because the complexation between PEI and PSS was reported to be instantaneous, resulting in macrovoid formation. The longer phase separation time (>20 s) of CS and CMC could lead to the suppression of macrovoids.[41] However, the membrane prepared in the 1.0 M acetate buffer bath developed cracks on the surface with some random macrovoids in the cross-section (see Figures 2b and S5). This is probably because at higher buffer concentrations, the driving force for the phase separation between the polymer film and the acetate bath is very high, leading to rigid membranes that can develop cracks. In addition, the high viscosity of the casting solution and the hydrogen-bond interaction between the CMC and CS restrict the movement of the molecular chains, thus causing defects.

To determine the performance of the membranes, we first measured the pure water permeability using a dead-end filtration cell setup. The water permeability was tested at a pressure of 1 bar, and all the membranes were stable at this pressure during the test. The results are shown in Figure 3. As

https://doi.org/10.1021/acsapm.2c01901
ACS Appl. Polym. Mater. 2023, 5, 1810−1818

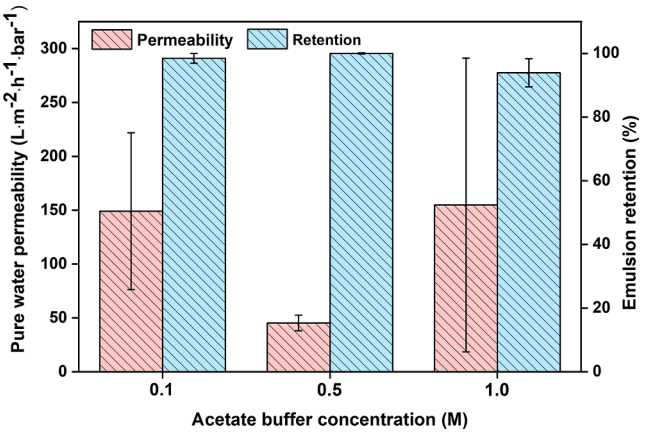

Figure 3. Pure water permeability and *n*-hexadecane-in-water emulsion retention of the membranes prepared in different concentrations of acetate buffer in the coagulation bath. The pH of the buffer bath was 5. All measurements were done in triplicate; the error bar represents the standard deviation.

expected, the porous membranes showed higher water permeabilities. The membrane prepared in the 0.1 M acetate buffer bath had a permeability of ∼149 $L{\cdot}m^{-2}{\cdot}h^{-1}{\cdot}bar^{-1}$ because of its porous surface as well as inner structure, which is in accordance with Figure 2a. In comparison, the relatively denser membrane, that is, the membrane prepared in the 0.5 M acetate buffer bath, had the lowest pure water permeability of ∼45 $L{\cdot}m^{-2}{\cdot}h^{-1}{\cdot}bar^{-1}$. When the acetate buffer concentration is further increased to 1.0 M, although the membrane showed a denser top surface, the pure water permeability increased to ∼155 $L{\cdot}m^{-2}{\cdot}h^{-1}{\cdot}bar^{-1}$. The increase is likely due to the cracks on the surface at higher pressure allowing easy water transport. Besides the absolute values, variations between samples as shown by the error bar also gave information on the structure of the membranes. The membranes prepared in the 0.1 M bath showed a large error bar due to the porous structure, while the much more homogeneous and dense structure of the membrane prepared in the 0.5 M bath had a small error bar. On the other hand, the largest error bar appeared for the membranes prepared in a 1.0 M buffer bath where the cracks and macrovoids in the membrane caused the large variation between different samples, explaining nonuniform permeabilities.

We further investigated the influence of acetate buffer concentration on the retention performance of the membranes using the same dead-end filtration cell setup. The *n*-hexadecane-in-water emulsion was used with an average droplet size of 3−4 μm. As shown in Figure 3, all the membranes exhibited a high retention (>94%) of the *n*-hexadecane-in-water droplets. The membranes prepared in 0.1 and 0.5 M baths showed retentions of ∼98 and ∼99%, respectively. For both membranes, the pore diameter of the membrane top layer was capable of retaining the emulsion droplets. For the membrane prepared in a 1.0 M buffer bath, it showed a retention of just ∼94%, possibly because of the defects in the membranes. Clearly, it is possible to prepare membranes completely based on bio-based polyelectrolytes using the APS approach. The membranes act as microfiltration membranes and are able to effectively remove oil from an oil-in-water emulsion. The concentration of the acetate buffer solution provides a relevant tuning parameter, although too fast coagulation does lead to the formation of defects.

3.3. Effect of the Acetate Buffer pH. Besides the acetate buffer concentration, the pH of the coagulation bath is also expected to play an important role in the structure and thus the performance of the complex membranes.[9] In this work, acetate buffer baths at pH 4.5, 5.0, and 5.5 were prepared separately. The concentration of the baths was kept at 0.5 M because at this concentration, the phase separation process was quick and the resulting membrane exhibited a stable structure with a dense top surface and porous cross-section. Besides, the membranes showed low pure water permeability and high oil droplet retention. Stable and intact membranes were obtained at all of the pH values of the coagulation bath, see photographs in Figure S7. With the increase of bath pH, the complexation process of the membranes became faster. Similar to the research on the influence of the acetate buffer concentration, we first observed the membrane structure by SEM, and then the influence of buffer pH on the membrane permeability and retention performance was measured.

The structure of different membranes is shown in Figure 4. The membranes prepared in different pH baths showed dense top surfaces and porous cross-sections in general. In the membrane prepared in a pH 4.5 bath, small pores appeared on the surface (see Figure 4a), indicating that the precipitation rate was already leading to a denser pore structure.[9] With the further increase in bath pH to 5.0 and 5.5, fewer pores were

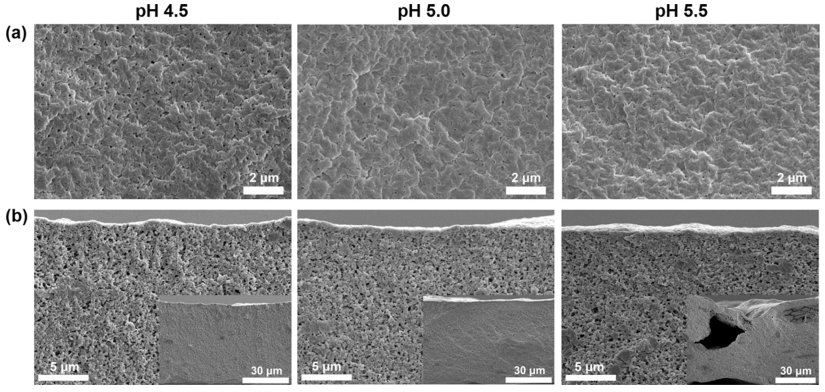

Figure 4. SEM images of membranes: (a) top surface (10,000× magnification) and (b) cross-section (5000× magnification) prepared in different pH (pH 4.5, 5.0, and 5.5) acetate buffer coagulation baths. The magnifications of the inset images are 1500× (pH 4.5 and 5.5) and 1300× (pH 5.5). The concentration of the buffer bath was 0.5 M.

https://doi.org/10.1021/acsapm.2c01901
ACS Appl. Polym. Mater. 2023, 5, 1810−1818

seen on the surface. However, cracks appeared in the membrane prepared in a pH 5.5 bath. The pore diameter distribution can be seen in Figure S9. The membranes prepared in pH 4.5, 5.0, and 5.5 baths showed average pore diameters of 89, 80, and 75 nm, respectively. All the membranes prepared in different pH baths showed a similar sponge-like morphology in the cross-section with no obvious differences (see Figure 4b). Similar to the membranes prepared in different concentrations of buffer baths, the cross-section of the membranes showed a dense layer near the top surface. However, the thickness of the dense layers did not show an obvious increase with the increase in bath pH. What is more, the structures of these membranes are very similar to those of NIPS membranes obtained via spinodal decomposition.[41,42] However, there were also random cracks appeared on the surface and macrovoids developed in the cross-section of the membrane prepared in the pH 5.5 bath (see Figures 4b and S8). As explained before, the membrane prepared in the bath of 1.0 M acetate buffer not only had smaller pores but also contained defects due to the fast phase separation. Similarly, for the membrane prepared in a pH 5.5 bath, the pH difference between the casting film (pH ∼1) and the coagulation bath was higher, leading to a rapid rate of precipitation which ultimately resulted in the formation of macrovoids in the substructure.

From Figure 5, it is evident that the membranes prepared in pH 4.5 and pH 5.0 baths exhibited comparable pure water

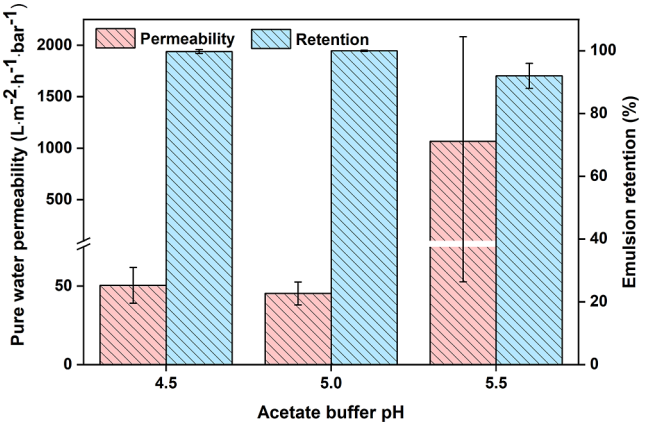

Figure 5. Pure water permeability and *n*-hexadecane droplet retention of the membranes prepared in different pH of the acetate buffer in coagulation baths. The concentration of the buffer bath was 0.5 M. All measurements were done in triplicate; the error bar represents the standard deviation.

permeabilities of ∼50 and ∼45 $L{\cdot}m^{-2}{\cdot}h^{-1}{\cdot}bar^{-1}$, respectively. Although there were more pores on the top surface of the membrane prepared in the pH 4.5 bath, the membranes prepared in pH 4.5 and 5.5 baths had relatively similar pore diameters of 89 and 80 nm, respectively, see Figure S9. Meanwhile, the *n*-hexadecane-in-water emulsion droplet retentions for the membranes prepared in pH 4.5 and pH 5.0 baths were both above 99%. When the bath pH was increased to 5.5, the obtained membrane exhibited a much higher pure water permeability of ∼1067 $L{\cdot}m^{-2}{\cdot}h^{-1}{\cdot}bar^{-1}$. Besides, the error bar of the permeability was very large, again indicating the presence of defects. In the pH 5.5 bath, the high driving force not only caused rapid complexation between CMC and CS but also caused inhomogeneity and defects as a result of the limited polymer mobility inside the membrane. The membrane still showed an oil droplet retention of higher than 90%, which means the defects are significantly smaller than the size of the oil droplet. Compared to the oil−water separation membranes in the literature, the membranes prepared in this work showed comparable separation ability but at lower permeability, which should be improved in the future.[43−46]

3.4. Mechanical Property and Stability of the Membranes. The membranes prepared in the pH ∼5, 0.5 M acetate buffer bath were chosen to evaluate their mechanical property and stability. Since the membranes were developed for pressure-driven processes, the mechanical strength was first quantified by operating the membranes at elevated feed pressures. The feed water pressure was gradually increased from 1 to 4 bar with an increment of 1 bar until a steady-state permeation was achieved. The pure water permeability at each pressure was recorded, and the results are shown in Figure S10. As evident, there was only a slight increase in the water permeability when the pressure was increased to 4 bar. Therefore, the results suggest that the membranes are mechanically stable and retain their water permeabilities until 4 bar of applied water pressure. Typical microfiltration membranes are generally operated at a less feed pressure of <4 bar.[47] To further quantitatively characterize the mechanical property, we also measured the tensile strength of the membranes using an electromechanical testing system, Instron 5800. First, the membranes (prepared in pH ∼5, 0.5 M acetate buffer baths) were cut into 50 × 5 mm pieces. Then, the samples were taken out from water, and the excess water was immediately removed before the measurement. At least three samples were measured at room temperature at a strain rate of 2 $mm{\cdot}min^{-1}$. The membranes showed an average Young's modulus of 4.29 ± 0.77 MPa, an elongation of break of 6.84 ± 0.22%, and a tensile stress of 0.22 ± 0.05 MPa. Although these values are not high, the membranes were sufficiently mechanically stable for microfiltration applications.

To study the pH stability of the membranes, we also chose the membranes prepared in the pH 5, 0.5 M acetate buffer bath and then placed the membranes in aqueous solutions at different pH values (pH 2, 5, 6, 8, 10, and 12). After 12 days, the membranes were taken out and washed with deionized water totally, and then their pure water permeability was tested. As shown in Figure S11, the membrane placed in the solution of pH 2 swelled a lot. At this pH, CMC became partly charged, so there were less charge pairs between the polyelectrolytes, leading to less complexation. Although the membrane recovered a lot after washing with water, the membrane structure was more compacted because of the reconstitution of polyelectrolyte chains, which showed a much lower pure water permeability (see Figure S12). The membranes placed at pH 5 to pH 8 solutions were stable and did not show significant morphology changes. The membrane placed in the pH 5 solution showed a somewhat higher pure water permeability, perhaps due to the membrane swelling. Besides, the membranes placed at pH 6 and pH 8 had consistent pure water permeability compared to the freshly prepared membranes. However, the membranes were not stable when the pH was above 10, and the structures could not recover after washing with water, perhaps because the chitosan was uncharged.

The salt stability of the membranes was evaluated by placing the membranes in 0.5 and 1.0 M sodium chloride solutions for

https://doi.org/10.1021/acsapm.2c01901
ACS Appl. Polym. Mater. 2023, 5, 1810−1818

5 days; the pure water permeability after washing with water was also measured. As shown in Figures S13 and S14, the membranes did not show significant morphology changes after being placed in sodium chloride solutions for 5 days. After washing with water, the membrane placed in a 0.5 M sodium chloride solution was still stable and showed a slightly decreased pure water permeability. However, the membrane placed in a 1.0 M sodium chloride solution swelled after washing with water, and its permeability decreased a lot, which was probably because the membrane structure has been changed at 1.0 M salt concentration for 5 days.

3.5. Comparison of APS Membranes Based on Synthetic and Bio-Based Polyelectrolytes. The structure and performance results have confirmed the possibility to prepare polyelectrolyte complex membranes through the APS approach by using natural/bio-based polyelectrolytes. Compared to the previous work that used synthetic polyelectrolytes, natural polyelectrolytes such as CMC and CS are more sustainable because they are obtained from natural sources and are economic. Therefore, the prepared membranes have more potential to be used in not only water treatment but also medicine or food fields. However, there are some limitations to using CMC and CS.

First, because of the high viscosity of the CS solution, it is difficult to prepare a casting solution of higher concentrations. Therefore, it increases the difficulty to improve the mechanical stability of the CMC−CS membranes. At the same time, it is found that the batches of CS products influence the experiments a lot because of the difference in deacetylation degree and the sources. It may be a general problem for bio-based polyelectrolytes. Besides, the crosslinking method in the APS process, for example, glutaraldehyde, cannot be used in this work because the introduction of glutaraldehyde would cause the membranes to become brittle and yellow. For now, the CMC-CS membranes have demonstrated the ability as microfiltration membranes to separate oil droplets from emulsions. However, the permeability of the membranes was low compared to that of the microfiltration membranes in the literature.[44,45,48] In the future, the performance of the CMC−CS membrane will be improved by employing a suitable crosslinker or combining with other materials. Additionally, sustainable polyelectrolyte complex membranes based on other natural polyelectrolytes, such as sodium alginate, will be prepared by the APS approach. What is more, we will also focus on preparing more biocompatible complex membranes that can be used in medical application.

4. CONCLUSIONS

In this work, bio-derived polyanionic CMC and polycationic CS were successfully used to prepare polyelectrolyte complex membranes by the pH-change-induced APS approach. The monomer mixing ratios were first optimized to obtain a homogeneous casting solution. It was found that the casting solution with the CMC/CS mixing ratio of 1:1 and pH ∼1 resulted in mechanically stable membranes. Furthermore, the concentration and pH of the acetate buffer coagulation baths were varied to study the influence on the membrane structure and performance. The results revealed that increasing the acetate buffer concentration from 0.1 to 1.0 M led to higher driving force for complexation and subsequently faster phase separation, resulting in asymmetric membranes having a more obvious dense top layer. The membrane prepared in the 0.1 M buffer bath had an irregular porous top surface, while the membranes prepared in 0.5 and 1.0 M buffer baths showed significantly denser surfaces. The membranes showed tunable pure water permeabilities in the range of 45−155 $L{\cdot}m^{-2}{\cdot}h^{-1}{\cdot}bar^{-1}$ with an oil droplet retention of ∼94−99%. Finally, the effects of acetate buffer pH were investigated by casting membranes at pH 4.5−5.5. All the membranes showed dense top surfaces and porous cross-sections in general. It was also found that the higher pH led to smaller pores due to faster deprotonation of CMC and the subsequent complexation with CS. The membranes prepared in pH 4.5 and 5.0 baths exhibited comparable pure water permeabilities of ∼50 and ∼45 $L{\cdot}m^{-2}{\cdot}h^{-1}{\cdot}bar^{-1}$ with an emulsion droplet retention of ∼99%. However, the membrane prepared in the pH 5.5 bath showed a pure water permeability of ∼1067 $L{\cdot}m^{-2}{\cdot}h^{-1}{\cdot}bar^{-1}$ which was attributed to microcracks that appeared at operating pressure. This work confirms that bio-derived polyelectrolytes can indeed be used to prepare more sustainable APS membranes which can potentially be used in water treatment applications. In the future, other natural/bio-derived polyelectrolytes could be used to prepare complex membranes having interesting separation properties.

■ ASSOCIATED CONTENT

Supporting Information

The Supporting Information is available free of charge at https://pubs.acs.org/doi/10.1021/acsapm.2c01901.

Photographs of CS solutions; photographs of CMC−CS solutions and membranes with different monomer ratios; photographs, SEM images, and pore diameter distribution of membranes prepared at different concentrations and pH of acetate buffer coagulation baths; pure water permeability of membranes measured at increased feed pressure; and photographs and pure water permeability of the membranes after being treated with different pH and NaCl concentration solutions (PDF)

■ AUTHOR INFORMATION

Corresponding Author

Saskia Lindhoud − *Faculty of Science and Technology, Department of Molecules & Materials, MESA+ Institute for Nanotechnology, University of Twente, Enschede 7500 AE, The Netherlands;* orcid.org/0000-0002-4164-0763; Email: s.lindhoud@utwente.nl

Authors

Lijie Li − *Faculty of Science and Technology, Department of Molecules & Materials, MESA+ Institute for Nanotechnology, University of Twente, Enschede 7500 AE, The Netherlands; Faculty of Science and Technology, Membrane Science and Technology, MESA+ Institute for Nanotechnology, University of Twente, Enschede 7500 AE, The Netherlands*

Muhammad Irshad Baig − *Faculty of Science and Technology, Membrane Science and Technology, MESA+ Institute for Nanotechnology, University of Twente, Enschede 7500 AE, The Netherlands;* orcid.org/0000-0002-7636-0630

Wiebe M. de Vos − *Faculty of Science and Technology, Membrane Science and Technology, MESA+ Institute for Nanotechnology, University of Twente, Enschede 7500 AE, The Netherlands;* orcid.org/0000-0002-0133-1931

Complete contact information is available at: https://pubs.acs.org/10.1021/acsapm.2c01901

Notes

The authors declare no competing financial interest.

■ ACKNOWLEDGMENTS

L.L. appreciates the Chinese Scholarship Council (CSC) for providing a scholarship (CSC PhD Fellowship no. 202006630012 to L.L.). The authors acknowledge Jéré J. van Lente for the support in experiments.

■ REFERENCES

(1) Lee, A.; Elam, J. W.; Darling, S. B. Membrane materials for water purification: Design, development, and application. *Environ. Sci.: Water Res. Technol.* **2016**, *2*, 17−42.
(2) Baker, R. W. *Membrane Technology and Applications*; John Wiley & Sons, 2012, pp 1−575.
(3) Nunes, S. P.; Peinemann, K.-V. *Membrane Technology: In the Chemical Industry*; John Wiley & Sons, 2006, pp 1−340.
(4) Guillen, G. R.; Pan, Y.; Li, M.; Hoek, E. M. Preparation and characterization of membranes formed by nonsolvent induced phase separation: A review. *Ind. Eng. Chem. Res.* **2011**, *50*, 3798−3817.
(5) Figoli, A.; Marino, T.; Simone, S.; Di Nicolò, E.; Li, X.-M.; He, T.; Tornaghi, S.; Drioli, E. Towards non-toxic solvents for membrane preparation: A review. *Green Chem.* **2014**, *16*, 4034−4059.
(6) Meka, V. S.; Sing, M. K.; Pichika, M. R.; Nali, S. R.; Kolapalli, V. R.; Kesharwani, P. A comprehensive review on polyelectrolyte complexes. *Drug Discovery Today* **2017**, *22*, 1697−1706.
(7) Willott, J. D.; Nielen, W. M.; de Vos, W. M. Stimuli-responsive membranes through sustainable aqueous phase separation. *ACS Appl. Polym. Mater.* **2019**, *2*, 659−667.
(8) Durmaz, E. N.; Baig, M. I.; Willott, J. D.; de Vos, W. M. Polyelectrolyte complex membranes via salinity change induced aqueous phase separation. *ACS Appl. Polym. Mater.* **2020**, *2*, 2612−2621.
(9) Baig, M. I.; Sari, P. P. I.; Li, J.; Willott, J. D.; de Vos, W. M. Sustainable aqueous phase separation membranes prepared through mild pH shift induced polyelectrolyte complexation of PSS and PEI. *J. Membr. Sci.* **2021**, *625*, 119114.
(10) Kamp, J.; Emonds, S.; Borowec, J.; Restrepo Toro, M. A.; Wessling, M. On the organic solvent free preparation of ultrafiltration and nanofiltration membranes using polyelectrolyte complexation in an all aqueous phase inversion process. *J. Membr. Sci.* **2021**, *618*, 118632.
(11) Emonds, S.; Kamp, J.; Borowec, J.; Roth, H.; Wessling, M. Polyelectrolyte complex tubular membranes via a salt dilution induced phase inversion process. *Adv. Eng. Mater.* **2021**, *23*, 2001401.
(12) Sadman, K.; Delgado, D. E.; Won, Y.; Wang, Q.; Gray, K. A.; Shull, K. R. Versatile and high-throughput polyelectrolyte complex membranes via phase inversion. *ACS Appl. Mater. Interfaces* **2019**, *11*, 16018−16026.
(13) Baig, M. I.; Durmaz, E. N.; Willott, J. D.; Vos, W. M. Sustainable membrane production through polyelectrolyte complexation induced aqueous phase separation. *Adv. Funct. Mater.* **2020**, *30*, 1907344.
(14) Baig, M. I.; Willott, J. D.; de Vos, W. M. Tuning the structure and performance of polyelectrolyte complexation based aqueous phase separation membranes. *J. Membr. Sci.* **2020**, *615*, 118502.
(15) Durmaz, E. N.; Willott, J. D.; Fatima, A.; de Vos, W. M. Weak polyanion and strong polycation complex based membranes: Linking aqueous phase separation to traditional membrane fabrication. *Eur. Polym. J.* **2020**, *139*, 110015.
(16) Xu, D.; Hein, S.; Wang, K. Chitosan membrane in separation applications. *Mater. Sci. Technol.* **2008**, *24*, 1076−1087.
(17) Cabello, S. D. P.; Mollá, S.; Ochoa, N. A.; Marchese, J.; Giménez, E.; Compañ, V. New bio-polymeric membranes composed of alginate-carrageenan to be applied as polymer electrolyte membranes for DMFC. *J. Power Sources* **2014**, *265*, 345−355.
(18) Silva, M. A.; Bierhalz, A. C. K.; Kieckbusch, T. G. Alginate and pectin composite films crosslinked with Ca^{2+} ions: Effect of the plasticizer concentration. *Carbohydr. Polym.* **2009**, *77*, 736−742.
(19) Jiang, H.; Fang, D.; Hsiao, B. S.; Chu, B.; Chen, W. Optimization and characterization of dextran membranes prepared by electrospinning. *Biomacromolecules* **2004**, *5*, 326−333.
(20) Sadeghifar, H.; Venditti, R.; Jur, J.; Gorga, R. E.; Pawlak, J. J. Cellulose-lignin biodegradable and flexible UV protection film. *ACS Sustainable Chem. Eng.* **2017**, *5*, 625−631.
(21) Şen, F.; Uzunsoy, İ.; Baştürk, E.; Kahraman, M. V. Antimicrobial agent-free hybrid cationic starch/sodium alginate polyelectrolyte films for food packaging materials. *Carbohydr. Polym.* **2017**, *170*, 264−270.
(22) Costa, R. R.; Costa, A. M.; Caridade, S. G.; Mano, J. F. Compact saloplastic membranes of natural polysaccharides for soft tissue engineering. *Chem. Mater.* **2015**, *27*, 7490−7502.
(23) Thakur, V. K.; Voicu, S. I. Recent advances in cellulose and chitosan based membranes for water purification: A concise review. *Carbohydr. Polym.* **2016**, *146*, 148−165.
(24) Tian, B.; Liu, Y. Chitosan-based biomaterials: From discovery to food application. *Polym. Adv. Technol.* **2020**, *31*, 2408−2421.
(25) Zargar, V.; Asghari, M.; Afsari, M. Gas separation properties of swelled nanocomposite chitosan membranes cross-linked by 3-aminopropyltriethoxysilane. *Int. J. Environ. Sci. Technol.* **2019**, *16*, 37−46.
(26) Trang, T. T. C.; Takaomi, K. Chitosan and its biomass composites in application for water treatment. *Curr. Opin. Green Sustainable Chem.* **2021**, *29*, 100429.
(27) Xu, X.; Wang, L.; Guo, S.; Lei, L.; Tang, T. Surface chemical study on the covalent attachment of hydroxypropyltrimethyl ammonium chloride chitosan to titanium surfaces. *Appl. Surf. Sci.* **2011**, *257*, 10520−10528.
(28) Mivehi, L.; Hajir Bahrami, S.; Malek, R. M. A. Properties of polyacrylonitrile-N-(2-hydroxy) propyl-3-trimethylammonium chitosan chloride blend films and fibers. *J. Appl. Polym. Sci.* **2008**, *109*, 545−554.
(29) Tu, G.; Li, S.; Han, Y.; Li, Z.; Liu, J.; Liu, X.; Li, W. Fabrication of chitosan membranes via aqueous phase separation: Comparing the use of acidic and alkaline dope solutions. *J. Membr. Sci.* **2022**, *646*, 120256.
(30) Liuyun, J.; Yubao, L.; Chengdong, X. A novel composite membrane of chitosan-carboxymethyl cellulose polyelectrolyte complex membrane filled with nano-hydroxyapatite I. Preparation and properties. *J. Mater. Sci.: Mater. Med.* **2009**, *20*, 1645−1652.
(31) Park, S.; Choi, D.; Jeong, H.; Heo, J.; Hong, J. Drug loading and release behavior depending on the induced porosity of chitosan/cellulose multilayer nanofilms. *Mol. Pharm.* **2017**, *14*, 3322−3330.
(32) Chen, X.; Liu, J.; Feng, Z.; Shao, Z. Macroporous chitosan/carboxymethylcellulose blend membranes and their application for lysozyme adsorption. *J. Appl. Polym. Sci.* **2005**, *96*, 1267−1274.
(33) Zhao, Q.; Qian, J.; An, Q.; Gao, C.; Gui, Z.; Jin, H. Synthesis and characterization of soluble chitosan/sodium carboxymethyl cellulose polyelectrolyte complexes and the pervaporation dehydration of their homogeneous membranes. *J. Membr. Sci.* **2009**, *333*, 68−78.
(34) Chen, H.; Fan, M. Chitosan/carboxymethyl cellulose polyelectrolyte complex scaffolds for pulp cells regeneration. *J. Bioact. Compat. Polym.* **2007**, *22*, 475−491.
(35) Abdelbasset, W. K.; Elkholi, S. M.; Ismail, K. A.; AL-Ghamdi, H. S.; Mironov, S.; Ridha, H. S.; Maashi, M. S.; Thangavelu, L.; Mahmudiono, T.; Mustafa, Y. F. Mequinol-loaded carboxymethyl cellulose/chitosan electrospun wound dressing as a potential candidate to treat diabetic wounds. *Cellulose* **2022**, *29*, 7863−7881.
(36) Dickhout, J. M.; Kleijn, J. M.; Lammertink, R. G.; de Vos, W. M. Adhesion of emulsified oil droplets to hydrophilic and hydrophobic surfaces - effect of surfactant charge, surfactant concentration and ionic strength. *Soft Matter* **2018**, *14*, 5452−5460.
(37) Yeul, V. S.; Rayalu, S. S. Unprecedented chitin and chitosan: A chemical overview. *J. Polym. Environ.* **2013**, *21*, 606−614.

(38) Saïed, N.; Aïder, M. Zeta potential and turbidimetry analyzes for the evaluation of chitosan/phytic acid complex formation. *J. Food Res.* **2014**, *3*, 71.
(39) Wu, J.; Zhang, L. Dissolution behavior and conformation change of chitosan in concentrated chitosan hydrochloric acid solution and comparison with dilute and semidilute solutions. *Int. J. Biol. Macromol.* **2019**, *121*, 1101−1108.
(40) Vink, H. Acid-base equilibria in polyelectrolyte systems. *J. Chem. Soc., Faraday Trans. 1 Chem. Rec.* **1986**, *82*, 2353−2365.
(41) Strathmann, H.; Kock, K.; Amar, P.; Baker, R. The formation mechanism of asymmetric membranes. *Desalination* **1975**, *16*, 179−203.
(42) Nunes, S. P.; Inoue, T. Evidence for spinodal decomposition and nucleation and growth mechanisms during membrane formation. *J. Membr. Sci.* **1996**, *111*, 93−103.
(43) Dickhout, J. M.; Moreno, J.; Biesheuvel, P.; Boels, L.; Lammertink, R.; de Vos, W. Produced water treatment by membranes: A review from a colloidal perspective. *J. Colloid Interface Sci.* **2017**, *487*, 523−534.
(44) Baig, N.; Salhi, B.; Sajid, M.; Aljundi, I. H. Recent progress in microfiltration/ultrafiltration membranes for separation of oil and water emulsions. *Chem. Rec.* **2022**, *22*, No. e202100320.
(45) He, B.; Ding, Y.; Wang, J.; Yao, Z.; Qing, W.; Zhang, Y.; Liu, F.; Tang, C. Y. Sustaining fouling resistant membranes: Membrane fabrication, characterization and mechanism understanding of demulsification and fouling-resistance. *J. Membr. Sci.* **2019**, *581*, 105−113.
(46) Ang, M. B. M. Y.; Devanadera, K. P. O.; Duena, A. N. R.; Luo, Z.-Y.; Chiao, Y.-H.; Millare, J. C.; Aquino, R. R.; Huang, S.-H.; Lee, K.-R. Modifying cellulose- acetate mixed-matrix membranes for improved oil-water separation: Comparison between sodium and organo-montmorillonite as particle additives. *Membranes* **2021**, *11*, 80.
(47) Charcosset, C. *Membrane Processes in Biotechnology and Pharmaceutics*; Elsevier, 2012, pp 1−336.
(48) Gao, J.; Wang, J.; Xu, Q.; Wu, S.; Chen, Y. Regenerated cellulose strongly adhered by a supramolecular adhesive onto the PVDF membrane for a highly efficient oil/water separation. *Green Chem.* **2021**, *23*, 5633−5646.

https://doi.org/10.1021/acsapm.2c01901
ACS Appl. Polym. Mater. 2023, 5, 1810−1818